Title

Investigation of the competition between Tl+ and Ce3+ scintillation in Tl2LiYCl6:Ce, an elpasolite scintillator

Authors

Moretti, Federico
Onken, Drew
Perrodin, Didier
et al.

Publication Date

2022

DOI

10.1016/j.jlumin.2021.118549

Peer reviewed

Journal of Luminescence 241 (2022) 118549

Contents lists available at ScienceDirect

Journal of Luminescence

journal homepage: www.elsevier.com/locate/jlumin

Investigation of the competition between Tl^{+} and Ce^{3+} scintillation in Tl_2LiYCl_6:Ce, an elpasolite scintillator

Federico Moretti *, Drew Onken, Didier Perrodin, Edith Bourret

Lawrence Berkeley National Laboratory, Cyclotron Road, Berkeley, CA, 94720, USA

ARTICLE INFO

Keywords:
Tl_2LiYCl_6
Single crystals
Scintillator
Luminescence
Ce^{3+}

ABSTRACT

Li-containing elpasolite scintillators are currently investigated for their ability to detect both thermal neutrons and gamma photons with a single inorganic crystal. The scintillation is typically triggered by using an activator such as Ce. However, when Tl, also a luminescent ion, is present in the matrix, competition between the two centers Tl and Ce can occur. In this study, we are using Ce doped Tl_2LiYCl_6 to investigate this competition. To this end, the Ce (which substitutes Y) concentration is varied from 0 to 1 in the $Tl_2LiY_{1-x}Ce_xCl_6$ composition. In the low concentration range in which Ce remains a dopant, the photo- and radioluminescence spectra show that the scintillation of Tl_2LiYCl_6:Ce is mostly dominated by recombination on intrinsic luminescent centers. For cerium concentrations higher than x = 0.02, very different emissions can be easily distinguished from the photo- and radioluminescence of undoped and low Ce doped Tl_2LiYCl_6 crystals. These emissions are attributed to the formation of a second phase Tl_2CeCl_5, identified by X-ray diffraction. We conclude that the intrinsic luminescence related to Tl dominates the scintillation in the range of concentration for which Ce does substitute on the Y-site.

1. Introduction

Li-containing elpasolite scintillators are currently investigated for their ability to detect both thermal neutrons and gamma photons with a single inorganic crystal. Cs_2LiYCl_6:Ce (CLYC:Ce), in particular, is already a commercial product [1] and shows good performance on both neutron/gamma discrimination and light yield [2–7]. The preponderance of light elements, however, limits the effective atomic number (Z_{eff}) and the density of this matrix to the detriment of the photo-fraction of detected gamma events.

The substitution of Cs for Tl allows to increase the Z_{eff} (from 45 to 69) and the density (from 3.3 to 4.5 g/cm^3). This new Tl_2LiYCl_6 (TLYC) elpasolite was reported [8–10] and showed a light yield of about 27,000 ph/MeV for gammas, compared to CLYC 18,000 ph/MeV, and a good energy resolution of about 4%. However, a slight reduction in the gamma/neutron discrimination has also been observed [10]. We note that Tl is an efficient emitter in itself and TLYC is an intrinsic scintillator. However, by analogy to CLYC, in most of the published results TLYC crystals are activated with Ce^{3+}, but only reporting on a few Ce concentrations. Ariesanti et al. [11], in particular, reported results for a series of TLYC crystals with Ce concentrations in the 0–9 mol% range. The reported radioluminescence (RL) spectra are characterized by a large and unstructured emission centered at about 430 nm, which shows rather little dependence on both shape and full width at half maximum on the Ce content. This is in contrast to what has been reported in the case of other elpasolites and CLYC, in particular, where the RL spectrum is strongly modified by the addition of cerium in the matrix [12]. Also the scintillation decay does not appear to be particularly affected by the Ce concentration [8–10], since it is always a multi-exponential decay with rather long characteristic decay times of several hundred and few thousand nanosecond main components. These are accompanied by a generally very weak fraction of a few tens of nanoseconds whose intensity ratios do not substantially change upon Ce concentration modification. Therefore, the role of Ce^{3+} in the scintillation and, more in general, on the optical properties of TLYC is not clear.

In this paper, we investigate the luminescence properties of $Tl_2LiY_{1-x}Ce_xCl_6$ single crystals for various cerium concentrations ranging from x = 0 (undoped) to x = 1 (full yttrium substitution) in order to clarify the role of Ce in the TLYC scintillation and optical properties. X-ray diffraction measurements have also been performed to clarify the possible presence of segregation phenomena and the formation of secondary phases.

* Corresponding author.
E-mail address: fmoretti@lbl.gov (F. Moretti).

https://doi.org/10.1016/j.jlumin.2021.118549
Received 21 May 2021; Received in revised form 15 September 2021; Accepted 21 October 2021
Available online 22 October 2021

2. Experimental

$Tl_2LiY_{1-x}Ce_xCl_6$ single crystals were grown with the Bridgman-Stockbarger method in evacuated sealed quartz ampoules using high purity LiCl, TlCl, YCl_3, and $CeCl_3$ beads from APL Engineered Materials and EMD Performance Materials. The crystals were grown starting from stoichiometric mixtures of the raw materials and with Ce concentration x equal to 0, 0.005, 0.015, 0.02, 0.03, 0.05, 0.1, 0.2, 0.6, and 1. Considering the hygroscopicity of both raw materials and grown crystals, all material handling was performed in argon-filled glove boxes maintained below 0.1 ppm of O_2 and H_2O. Prior to ampoule sealing, the raw materials were heated up to 110 °C and kept under vacuum (~10^{-6} Torr) for at least 24 h. All crystals were grown at a rate of 1 mm/h.

Phase identification was performed by powder x-ray diffraction using a D2 Phaser X-ray diffractometer (Bruker) with Cu Kα radiation. Parts of the obtained crystals were crushed into smaller pieces (0.2–2 mm) and put into gas-tight quartz cuvettes for the optical characterization.

Room temperature radioluminescence (RL) measurements were obtained using a Bruker FR591 x-ray generator operating at 50 kV as excitation source. The light emitted by the samples was collected by a SpectraPro-2150i spectrometer (Acton Research) coupled to a Pixis:1008 CCD detector (Princeton Instruments). The obtained spectra have been corrected for the instrumental response. The same light detection system was also used to collect photoluminescence excitation (PLE) and emission (PL) patterns: in this case a 75 W Xe-lamp, coupled to a monochromator (SpectraPro-2150i Acton Research) for spectral selection, was used as excitation source. Both excitation and emission spectra have been corrected for the instrument response.

A custom build pulsed X-ray system working in time correlated single photon counting (TCSPC) and consisting of a light-excited x-ray tube (Hamamatsu N5084) driven by an ultrafast Ti:sapphire laser (200 fs pulses, Coherent Mira) and a Hamamatsu multichannel plate photomultiplier (R3809U-50) was used to collect scintillation decay measurements. No wavelength discrimination was used to select the light emitted by the samples. The signal is processed through an Ortec 9308 ps analyzer. The overall instrument response function (IRF) of the system is of the order of few hundred of ps as full width at half maximum (FWHM) [13]. The decay times were determined from the experimental results using the method described in reference [14].

A Horiba Jobin-Yvon Fluorolog-3 spectrofluorometer working in TCSPC was used to obtain photoluminescence decay measurements. The excitation was done using three different pulsed diodes (NanoLED, Horiba) with emission wavelength at 268, 311, and 375 nm and FWHM of 10 nm. The system IRF is 1.6 ns as FWHM. Fits of the luminescence decays were performed with Horiba DAS6 software considering the convolution of the signal with the IRF.

3. Results and discussion

3.1. Growth results

Fig. 1 reports a few examples of $Tl_2LiY_{1-x}Ce_xCl_6$ crystals for different Ce concentrations. As it is clearly visible, the transparency of the grown crystals decreases as the concentration of Ce is increased. The loss of transparency starts to become evident for Ce concentrations higher than x = 0.05, with the samples becoming completely opaque for the full substitution of Y with Ce.

X-ray diffraction measurements for all samples were performed to clarify the reason for the reduced transparency of the grown crystal upon increase of Ce content. The results are presented in Fig. 2. At low concentrations, lower than 10 mol% (x = 0.1), the diffractograms are consistent with those of pure pseudocubic $P4_2$ structure TLYC [9,15]. As the Ce concentration is increased, several new peaks appear and are particularly evident at 2θ angles 22°–24°, 30.5°–32°. These new diffraction components are not related to the TLYC crystal structure, but rather to the presence of Tl_2CeCl_5 (TCC) phase (orthorhombic *Pnma* crystal structure, similar to Tl_2LaCl_5 [16]) that formed during the crystal growth. Indeed, the nominally grown $Tl_2LiCeCl_6$ crystal present a diffraction pattern that is identical to that of TCC. The segregation of TCC from the $Tl_2LiY_{1-x}Ce_xCl_6$ should lead to the formation of either Li-rich phases or, directly, LiCl. In the case of the full Ce substitution,

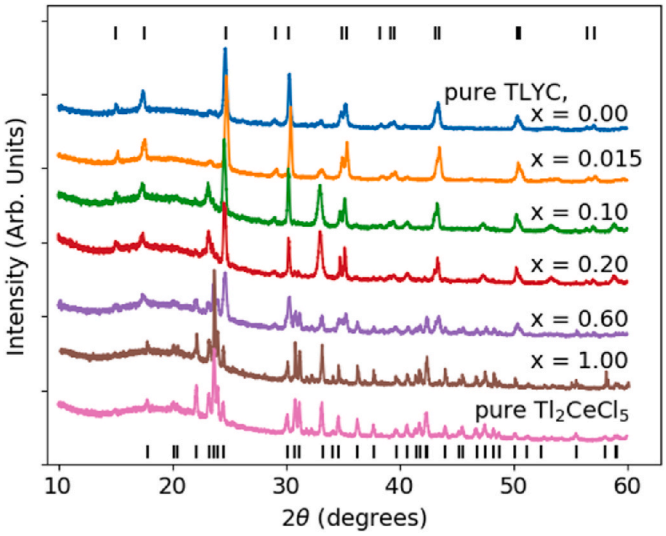

Fig. 2. X-ray diffraction curves for the $Tl_2LiY_{1-x}Ce_xCl_6$ samples for different cerium concentrations in the x = 0 to 1 range. As a reference, also the Tl_2CeCl_5 diffractogram is reported. The small vertical lines at the bottom and the top of the figure mark the position of the main diffraction peaks of Tl_2CeCl_5 and of Tl_2LiYCl_6 crystals, respectively.

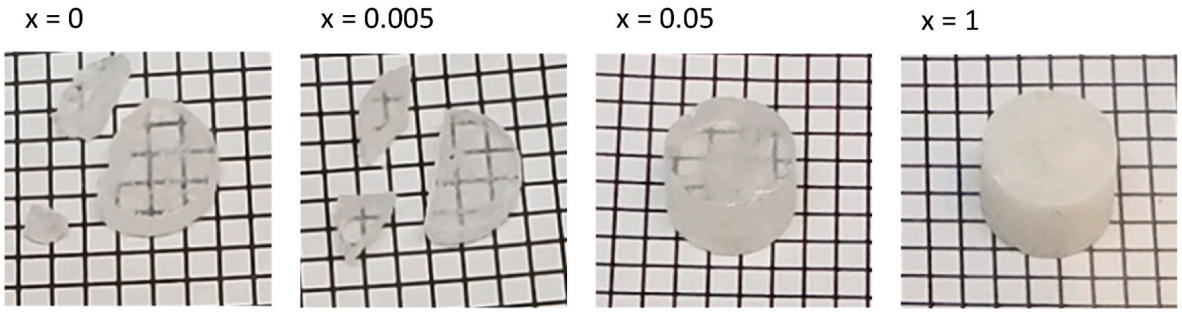

Fig. 1. Examples of $Tl_2LiY_{1-x}Ce_xCl_6$ polished single crystalline slices for different Ce concentrations after cutting from the related single crystal boules. The squares on the paper are 2 mm in size.

however, we have no clear evidence of the formation of LiCl phase, but it is hardly a surprise considering the presence of only light elements.

Considering these results, the following section dedicated to the optical properties of the investigated samples is subdivided in two parts, one for low Ce concentrations ($x < 0.02$) and the other for the higher concentrations for which the presence of the Tl_2CeCl_5 phase was detected.

3.2. Optical properties

3.2.1. Low Ce concentrations

Fig. 3 reports the RL spectra of TLYC without and with 1.5 mol% Ce ($x = 0.015$). The spectra are characterized by a main emission at about 430 nm accompanied by much weaker ones in the 280–350 nm region. The main emission is in very good agreement with the spectra reported in the literature [8,10] while the UV emissions have not been reported before. The differences between the spectra of two samples are quite subtle: the main emission of TLYC:Ce appears to be slightly larger than that of the undoped crystal, particularly on the long wavelength side of the emission peak. Moreover, the small UV contribution appears to be composed of two emissions instead of the one visible in the case of the undoped crystal, and they are also somewhat less intense. The discussion on the possible nature of these emission centers is reported below after the presentation of the steady state and time resolved photoluminescence results.

Scintillation time decay measurements, Fig. 4, of the undoped and 1.5 mol% doped TLYC have been performed to highlight differences in the decay profiles which cannot be obtained from the steady state RL spectra reported above. The decays of both the undoped and Ce doped samples are in rather good agreement with previously reported results [9,17] and are in both cases characterized by rather long-lived multi-exponential curves. The comparison between the two decays clearly evidences some variation among the weight and the decay time of the various components, which are reported in Table 1. Both sample decays are, however, dominated by components of the order of several hundreds of ns (which account for more than 80% of the total amount of light), while the faster (tens of ns) contributions are always a minority, even for the sample containing Ce^{3+}.

This comparison, together with the RL results above, suggests that Ce^{3+} is not the main radiative recombination center in the TLYC scintillation process. Other authors suggested, however, that the long scintillation decay times reported for TLYC:Ce are the result of a slow excitation transfer process from the matrix to the Ce^{3+} ions [9], similarly

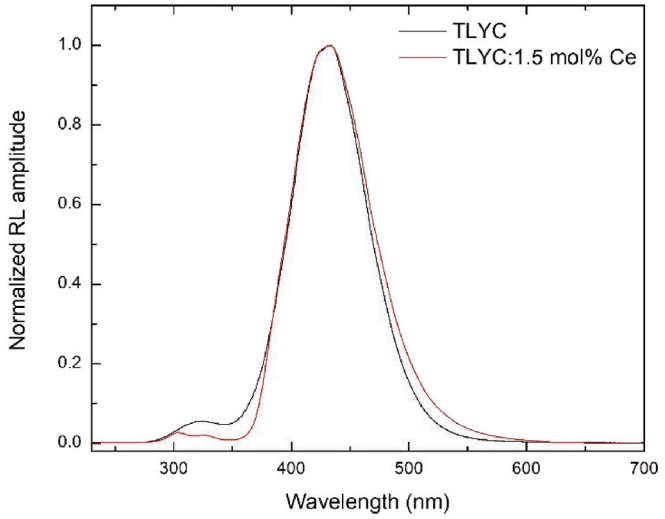

Fig. 3. Room temperature RL spectra of undoped and 1.5 mol% Ce-doped TLYC.

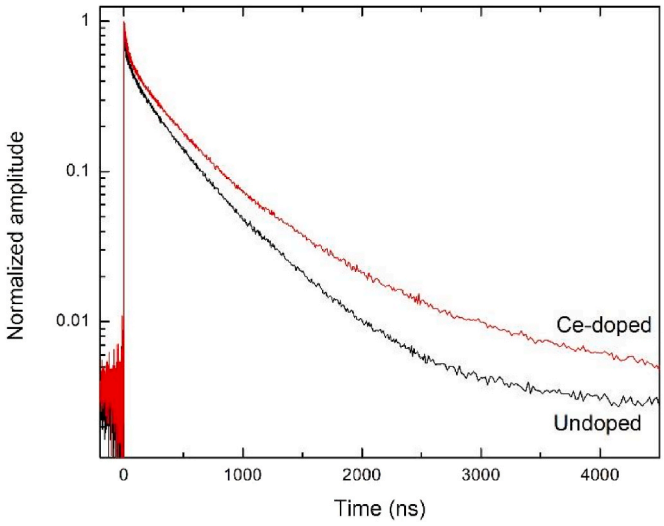

Fig. 4. Pulsed X-ray decay measurements obtained on undoped 1.5 mol% Ce doped LYC crystals.

Table 1
Results of fits in term of multiple exponential decay components of the pulsed X-ray decays reported in Fig. 4 for both TLYC and TLYC: 1.5 mol% Ce single crystals.

TLYC		TLYC:1.5 mol%Ce	
τ (ns)	Weight (%)	τ (ns)	Weight (%)
7	1	–	–
51	4	37	4
273	35	341	46
605	52	947	42

to what is observed in the case of other elpasolite scintillators [7,12,18].

PL measurements have been performed in order to clarify the RL results. The excitation/emission contour plot of TLYC and TLYC: 1.5 mol % Ce are reported in Fig. 5-A and B, respectively. Fig. 5-C reports the emission spectra of the two samples for selected excitation wavelengths and, as a comparison, the RL spectrum of TLYC. The PL excitation and emission pattern of TLYC shows only one excitation band that extends from 200 nm up to 260 nm which gives rise to emissions very similar to those detected in the RL measurement, see Fig. 5-C. On the contrary, the PL/PLE map of TLYC: 1.5 mol% Ce is characterized by a much more complicated behavior: again, excitation in the 200–260 nm range gives rise to an emission that is consistent with the PL and RL emissions detected in the case of the undoped TLYC. At longer excitation wavelengths (270–330 nm), the emission spectra become radically different with two main narrow emissions (at about 330 and 370 nm) accompanied by a much broader and less intense one centered at about 430 nm. This last contribution is excited also for longer wavelengths up to 370 nm. This latter contribution, although centered at the same wavelength of the emission excited in the deep UV, is also much larger, suggesting a possible different nature of the emitting center.

The occurrence in both TLYC and TLYC:Ce sample of the main emission excited in the 200–260 nm region suggests that this contribution is likely of intrinsic character. The two rather narrow emission visible for the TLYC:Ce sample are possibly related to the Ce^{3+} 5d to 4f radiative recombination, while the nature of the last contribution at longer excitation wavelengths is unclear, but it might be related to defects.

In view of these PL results, it seems clear that the RL emission observed in the case of TLYC:Ce is mainly composed of the intrinsic emission with only a weak contribution from the defect luminescence, thus explaining the larger long wavelength side of the RL spectrum. The

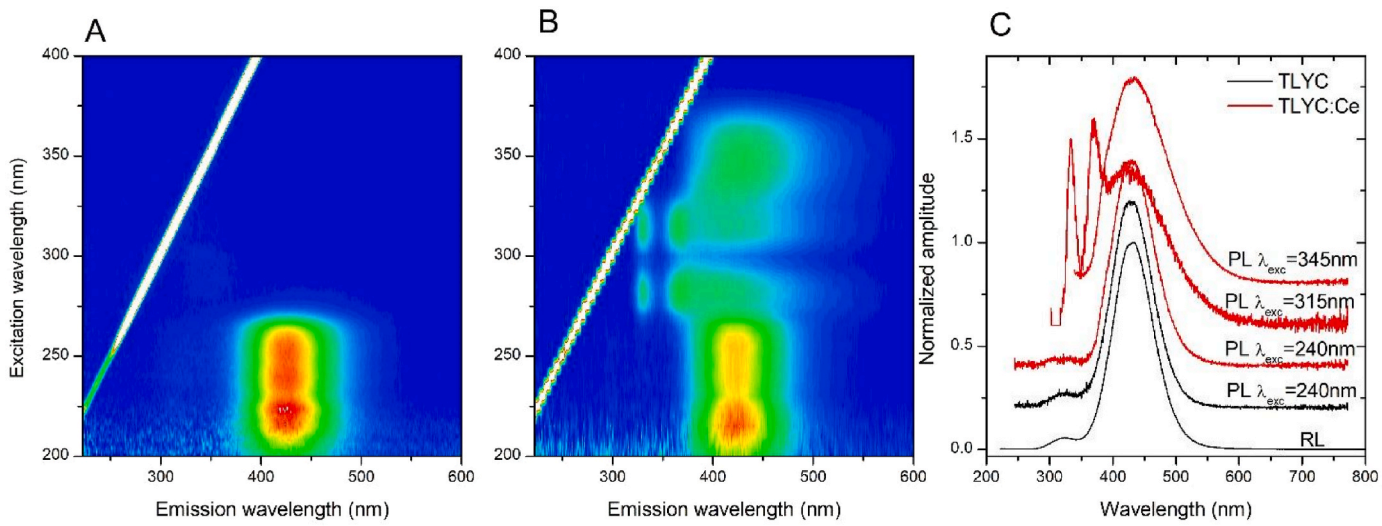

Fig. 5. PL excitation and emission contour plots of A) TLYC and B) TLYC: 1.5 mol% Ce. C) normalized PL emission spectra for selected excitation wavelengths of both TLYC and TLYC:Ce samples. As a reference, the RL emission spectrum of TLYC is reported as well. The curves have been shifted along the ordinate axis for clarity.

two narrow emissions clearly visible in PL are not evident in the RL spectrum, suggesting that their contribution to the RL is very limited if not negligible.

Fig. 6 reports the PL decays obtained on TLYC with excitation at 268 nm and emission at 325 and 420 nm which correspond to the weak UV emission and the main visible one, respectively, detected in both RL and PL measurements. The shorter wavelength emission is characterized by a PL decay composed by two contributions with decay times of about 13 and 410 ns (Table 2). On the contrary, the emission centered at 430 nm is characterized by a single exponential decay with decay time of the order of 490 ns. The longer decay component in the measurement at 325 nm might be still related to the main emission at 420 nm, since there is some overlap between the two emissions, as clearly visible in Fig. 5-C.

Fig. 7-A and B reports the photoluminescence decays of TLYC: 1.5 mol% Ce at two different emission wavelengths (335 and 420 nm, respectively) for different excitation wavelengths and representative of the observed trends in the luminescence decays. Results of fits in terms of exponential decay components of the experimental data are reported in Table 3 also for two other emission wavelengths (370 and 440 nm). The emissions at 335 and 370 nm are characterized by fast decays of the order of 13 ns, irrespective of the excitation wavelength. The 370 nm

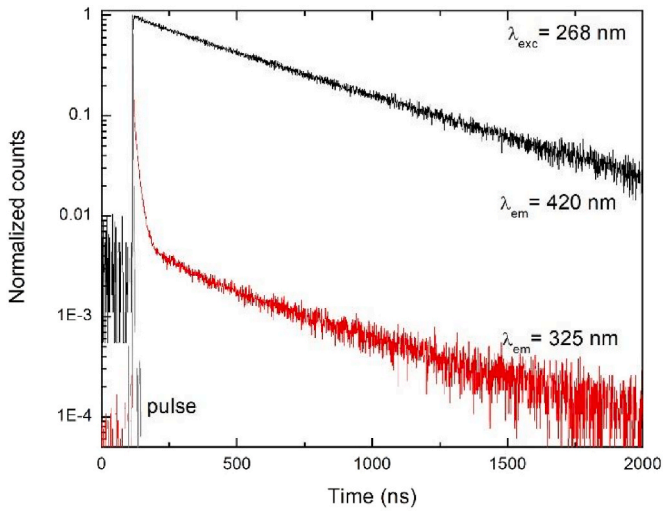

Fig. 6. Normalized PL decay measurements obtained on the undoped TLYC sample with excitation at 268 nm and emission at 325 nm and 420 nm.

Table 2
PL decay times of TLYC excited at 268 nm obtained by fits in terms of multiple exponential decay function. Errors on the obtained figures are of the order of few %.

Em. wavelength (nm)	τ_1 [ns] (weight [%])	τ_2 [ns] (weight [%])
325	13 (43)	410 (57)
420	–	486 (100)

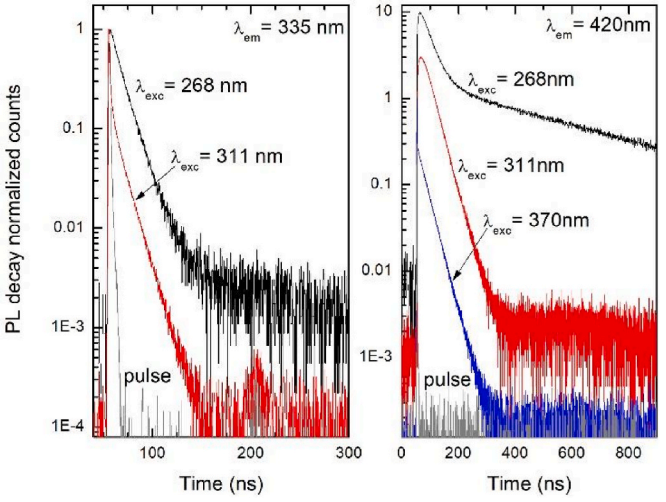

Fig. 7. Normalized PL decay of TLYC: 1.5 mol% Ce for emission wavelengths at 335 nm, left panel, and 420 nm, right panel. The right panel data have been shifted along the ordinate axis for clarity. Different excitation wavelengths, reported in the panels themselves, were used.

emission, however, presents also longer components with decay times of the order of 30 and 490 ns, and whose weights are dependent upon the excitation wavelength. In particular, the longest (490 ns) component is visible exclusively for the excitation at 268 nm, thus suggesting that these longer components are due to the spectral overlap between the narrow 370 nm emission and the larger ones above 400 nm. The 420 nm emission is characterized by a relatively fast component of about 30 ns, visible for all the excitation wavelengths, and a 490 ns one which is again visible only for the excitation at 268 nm. This emission is also

Table 3
TLYC: 1.5 mol% Ce PL decay results of fits performed in terms of multi-exponential decay components. Errors are of the order of few %.

Exc. Wavelength (nm)	Em. Wavelength (nm)	τ_1 [ns] (weight [%])	τ_2 [ns] (weight [%])	τ_3 [ns] (weight [%])
268	335	13 (88)		384 (12)
	370	13 (51)	36 (19)	499 (30)
	420	10 (risetime)	35 (41)	485 (59)
	450	10 (risetime)	37 (44)	482 (56)
311	335	12 (100)		
	370	12 (69)	33 (31)	
	420	10 (risetime)	35 (100)	
	440	10 (risetime)	35 (100)	
370	420		33 (100)	
	440		33 (100)	

characterized by a clear rise in intensity in the first 10 ns when the sample is excited at both 268 and 311 nm but not at 370 nm.

The time resolved PL data clearly reinforces the hypothesis of three distinct PL emitting centers in TLYC:Ce reported above in the discussion of the steady state PL spectra. The emission at 420 nm with excitation in the 200–260 nm region is characterized by a very long luminescence decay (about 490 ns) and is very similar, if not identical, to the one detected in the case of the undoped TLYC. This suggests, again, an intrinsic nature for this emission, although at the moment is not clear whether this contribution is due to some kind of self-trapped exciton or most likely to transitions among Tl^+ ion electronic levels.

The two narrow emissions at 330 and 370 nm have similar excitation pattern and luminescence decay times, suggesting a common nature: we can propose that the two emissions are related to Ce^{3+} ion transition between the excited 5d level and the two ground state 4f multiplets. The decay time (13 ns) of the two emission, however, is faster than the typical Ce^{3+} PL decays in this spectral region [19,20], suggesting that the Ce^{3+} 5d-4f electronic transitions are somewhat quenched. We cannot exclude that there might be also non-radiative energy transfer phenomena occurring between the Ce^{3+} ions and the centers responsible for the broad emission at 430 nm and excited in the 330–370 nm region. It also has to be noted that the energy difference between the 330 and 370 nm emission bands is somewhat large (about 2800 cm^{-1}) compared to the typical splitting (2200 cm^{-1}) among the $^2F_{5/2}$ and $^2F_{7/2}$ 4f multiplets of trivalent cerium [21], and that these two components appear quite narrow compared to the typical spectra of Ce^{3+} ions.

The third luminescence component, excited mainly in the 330–370 nm region and emitting at 430 nm, also has a fairly short luminescence decay (30 ns). The long decay contribution visible exclusively by excitation at 268 nm is, as already mentioned above, related to the intrinsic emission. This emission is also characterized by an evident rise in the luminescence amplitude that is possibly related to radiative energy transfer between the Ce^{3+} ions and this extrinsic radiative center. At the moment we do not have enough data to give a reasonable identification of the nature of this emitting center and we suppose, as already mentioned above, that it might be related to defects.

So far, only the main emission bands in both RL and PL of the two crystals were discussed. However, the RL spectra of the two crystals are clearly characterized by weak contributions in the 280–330 nm region. Similar emissions are also visible, albeit barely in the case of the Ce doped crystal, in the case of the PL emission spectra obtained at 240 nm as excitation wavelength. Considering the similar excitation and emission wavelength region, we can suppose that these contributions are due to the same emitting center in both the undoped and the Ce-containing samples and that this center is intrinsic in nature. The clear change in shape visible in the RL spectra might be due to the Ce^{3+} ion absorption contribution leading to partial reabsorption of the light emitted by this center. The nature of this center is, however, still unclear but it might be related, in analogy with the main emission at 430 nm, to fast singlet exciton recombination or transitions between Tl^+ 6sp and $6s^2$ electronic levels. The full investigation on the nature of this and of the main emission contribution is outside the scope of this work.

3.2.2. High Ce concentrations

The results reported above clearly show that Ce in low concentrations is not the dominant scintillation recombination center in TLYC. The interesting question is to see if the Ce emission can be increased by increasing its concentration. Unfortunately, as we reported above in section 3.1, increasing the Ce concentration results in the formation of the Tl_2CeCl_5 phase. This section is dedicated to the study of the luminescence properties of $TlLiY_{1-x}Ce_xCl_6$ for various high Ce concentrations up to the complete substitution of Y with Ce, and to determine the effect of the Tl_2CeCl_5 phase segregation on the optical characteristics of these samples.

The presence of the Tl_2CeCl_5 phase appears evidently in the luminescence characteristics. Fig. 8 reports the PL spectra of the nominally $Tl_2LiY_{1-x}Ce_xCl_6$ samples for Ce concentration in the x = 0.015 to 1 range. The spectra have been obtained by exciting the samples at 310 nm, one of the wavelengths that predominantly result in the Ce emission in the case of Ce as a dopant (see Fig. 5). The PL spectra show clearly the appearance of a further component centered at about 390 nm already for the sample doped with x = 0.02 Ce. This new component becomes the dominant luminescence feature for higher Ce concentrations, while the emissions related to Ce in the TLYC and the defect one quickly disappears. This new contribution is related to the Ce emission form the TCC phase: the PL emission spectrum of the $Tl_2LiCeCl_6$ and Tl_2CeCl_5 are in fact practically identical.

The RL spectra are affected as well by the presence of the TCC phase (Fig. 9), albeit to a lesser extent for Ce concentrations lower than x = 0.6. For concentrations lower or equal to 0.2, in fact, the spectrum is characterized by the main emission centered at about 430 nm, which has been already discussed above. However, as the Ce concentration increases a shoulder at about 390 nm becomes more and more evident, as clearly visible from the "bunching-up" of the curves toward 390 nm. For even higher concentrations, the main emission is at 390 nm, that is the main one of TCC. The different intensity ratio between the emission components obtained for PL and RL spectra as a function of Ce concentration is not surprising, considering that for X-ray irradiation the entirety of the matrix is excited while, on the contrary, the Ce ions are preferentially excited by the UV excitation.

PL and RL techniques also appear particularly sensitive, compared to

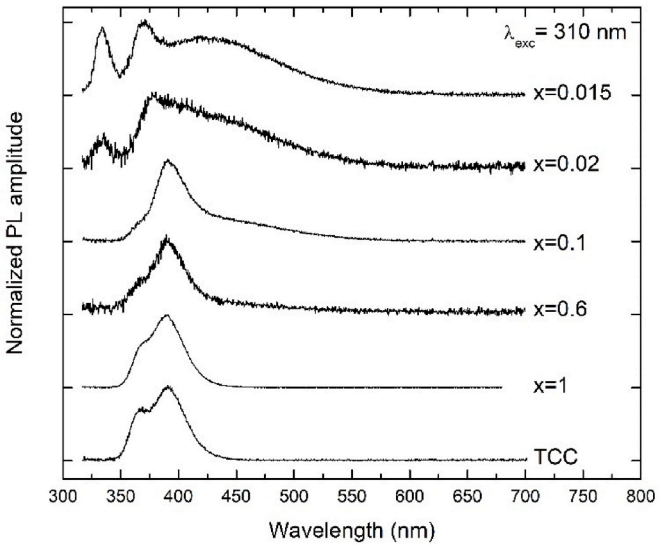

Fig. 8. PL spectra of $Tl_2LiY_{1-x}Ce_xCl_6$ for different Ce concentration and obtained by exciting the samples at 310 nm. The PL spectrum of Tl_2CeCl_5 (TCC) is also reported. The spectra have been shifted along the ordinate axis for clarity.

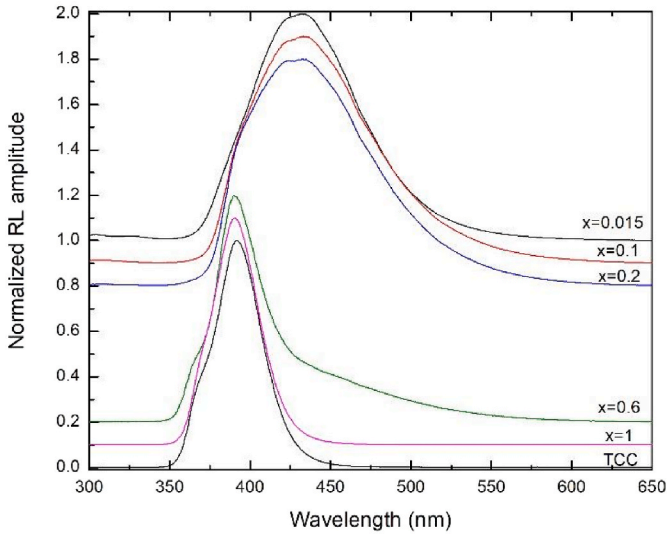

Fig. 9. RL spectra of $Tl_2LiY_{1-x}Ce_xCl_6$ samples for different Ce concentration reported in the figure. The spectra have been normalized to their maximum and shifted along the ordinate axis for clarity.

XRD, to the detection of comparatively small quantities of the TCC phase in TLYC, and they also allow us to reduce the Ce solubility limit estimated from XRD to less than x = 0.02.

4. Conclusions

The effect of Ce concentration on the optical properties of $Tl_2LiY_{1-x}Ce_xCl_6$ single crystals, obtained with the Bridgman-Stockbarger method, has been studied for Ce concentrations in the range $0 \leq x \leq 1$.

In the case of crystals in which cerium remains a substitutional ion in Tl_2LiYCl_6, the photoluminescence characterization shows the presence of three different emitting centers with remarkably different decay times. One is of intrinsic origin and is visible also in the case of the undoped crystal; the other two are instead possibly related to the specific Ce^{3+} 5d-4f recombination and to defect emission. The comparison between the photoluminescence and the radioluminescence results indicates that the radioluminescence spectrum detected in the case of Ce doped Tl_2LiYCl_6 is mostly composed by the intrinsic emission with a relatively small contribution related to defects. There are no indications of the Ce^{3+} related emission in radioluminescence.

XRD characterization indicates the formation of a secondary phase, Tl_2CeCl_5, for our sample with Ce concentration $x \geq 0.02$. The samples containing the Tl_2CeCl_5 phase are characterized by additional emission bands related to Ce^{3+} that are not present in the sample in which Ce^{3+} is substituted for Y in the Tl_2LiYCl_6 matrix. The high sensitivity of the photoluminescence and radioluminescence measurements allow to clearly distinguish the segregation of the Tl_2CeCl_5 phase for concentrations of cerium as low as x = 0.02.

Credit author statement

Federico Moretti: Investigation, Formal analysis, Visualization, Writing – original draft, writing –review & editing; **Drew Onken**: investigation, Data curation, Formal analysis, Visualization, Resources; **Didier Perrodin**: investigation, Resources; **Edith Bourret**: supervision, Project administration, Funding acquisition, Writing – review & editing

Declaration of competing interest

The authors declare that they have no known competing financial interests or personal relationships that could have appeared to influence the work reported in this paper.

Acknowledgement

This work was supported by the DOE SBIR project: RMD contract #DE-SC0015793 and was performed at Lawrence Berkeley National Laboratory under contract #AC02-05CH11231.

References

[1] Dynasil, Online catalog, https://www.dynasil.com/product-category/scintillators/clyc-gamma-neutron-scintillators/. May 2021.
[2] C.W.E. van Eijk, Inorganic scintillators for thermal neutron detection, IEEE Trans. Nucl. Sci. 59 (2012) 2342.
[3] J. Glodo, E. van Loef, R. Hawrami, W.M. Higgins, A. Churilov, U. Shirwadkar, K. S. Shah, Selected properties of Cs_2LiYCl_6, $Cs_2LiLaCl_6$, and $Cs_2LiLaBr_6$ scintillators, IEEE Trans. Nucl. Sci. 58 (2011) 334.
[4] J. Glodo, R. Hawrami, E. van Loef, U. Shirwadkar, K.S. Shah, Pulse shape discrimination with selected elpasolite crystals, IEEE Trans. Nucl. Sci. 59 (2012) 2328.
[5] L. Soundara-Pandian, J. Tower, C. Hines, P. O'Dougherty, J. Glodo, K. Shah, Characterization of large volume CLYC scintillators for nuclear security applications, IEEE Trans. Nucl. Sci. 64 (2017) 1744.
[6] A. Bessiere, P. Dorenbos, C.W. E van Eijk, K.W. Krämer, H.U. Güdel, Luminescence and scintillation properties of $Cs_2LiYCl_6:Ce^{3+}$ for γ neutron detection, Nucl. Instrum. Methods Phys. Res. 537 (2005) 242.
[7] C.M. Combes, P. Dorenbos, C.W.E. van Eijk, K.W. Krämer, H.U. Güdel, Optical and scintillation properties of pure and Ce^{3+}-doped Cs_2LiYCl_6 and $Li_3YCl_6:Ce^{3+}$ crystals, J. Lumin. 82 (1999) 299.
[8] H.J. Kim, G. Rooh, H. Park, S. Kim, $Tl_2LiYCl_6(Ce^{3+})$: new Tl-based elpasolite scintillation material, IEEE Trans. Nucl. Sci. 63 (2016) 439.
[9] G. Rooh, H.J. Kim, H. Park, S. Kim, Crystal growth and scintillation characterization of $Tl_2LiYCl_6:Ce^{3+}$, J. Cryst. Growth 459 (2017) 163.
[10] R. Hawrami, E. Ariesanti, L. Soundara-Pandian, J. Glodo, K.S. Shah, Tl_2LiYCl_6:Ce: a new elpasolite scintillator, IEEE Trans. Nucl. Sci. 63 (2016) 2838.
[11] E. Ariesanti, R. Hawrami, J. Finkelstein, H. Wei, L. Soundara-Pandian, J. Glodo, K. S. Shah, Effect of cerium concentration in Tl_2LiYCl_6 scintillation detectors, in: 2016 IEEE Nuclear Science Symposium, Medical Imaging Conference and Room-Temperature Semiconductor Detector Workshop, NSS/MIC/RTSD), Strasbourg, 2016.
[12] E.V.D. van Loef, P. Dorenbos, C.W.E. van Eijk, K.W. Krämer, H.U. Güdel, Scintillation and spectroscopy of the pure and Ce^{3+}-doped elpasolites: Cs_2LiYX_6 (X = Cl, Br), J. Phys. Condens. Matter 14 (2002) 8481.
[13] S.E. Derenzo, M.J. Weber, W.W. Moses, C. Dujardin, Measurements of the intrinsic decay times of common scintillators, IEEE Trans. Nucl. Sci. 47 (2000) 890.
[14] S.E. Derenzo, G.A. Bizarri, E. Bourret, R. Borade, Y. Eagleman, G. Gundiah, C. Rosen, 15 lutetium compounds screened for Ce^{3+} activated scintillation, Nucl. Instrum. Methods Phys. Res., Sect. A 908 (2018) 325.
[15] D.R. Onken, D. Perrodin, E.D. Bourret, S.C. Vogel, The crystal structure and temperature dependence of the elpasolite Tl_2LiYCl_6, J. Appl. Crystallogr. 54 (2021) 604.
[16] U. Shirwadkar, M. Loyd, M.-W. Du, E. van Loef, G. Ciampi, L. Soundara Pandian, L. Stand, M. Koschan, M. Zhuravleva, C. Melcher, K. Shah, Thallium-based scintillators for high-resolution gamma-ray spectroscopy: Ce^{3+}-doped Tl_2LaCl_5 and Tl_2LaBr_5, Nucl. Instrum. Methods Phys. Res. 962 (2020) 163684.
[17] R. Hawrami, E. Ariesanti, H. Wei, J. Finkelstein, J. Glodo, K. Shah, Tl_2LiYCl_6: large diameter, high performing, dual mode scintillator, Cryst. Growth Des. 17 (2017) 3960.
[18] P. Dorenbos, Scintillation mechanisms in Ce^{3+} doped halide scintillators, Phys. Status Solidi 202 (2005) 195.
[19] J.A. Mares, M. Nikl, C. Pedrini, B. Moine, K. Blazek, A study of fluorescence emission of Ce^{3+} ions in $YAlO_3$ crystals by the influence of doping concentration and codoping with Nd^{3+} and Cr^{3+}, Mater. Chem. Phys. 32 (1992) 342.
[20] Y. Pei, X.F. Chen, L.S. Qin, D.-M. Yao, G.-H. Ren, Temperature dependence of the luminescence properties of $LaCl_3$:Ce crystal, Chin. Phys. 15 (2006) 2756.
[21] G. Blasse and B.C. Grabmaier. Luminescent Materials, Springer Verlag, Berlin.